J Sol-Gel Sci Technol
DOI 10.1007/s10971-017-4394-z

Determination of the polymerization degree of various alkaline solutions: Raman investigation

L. Vidal[1] · A. Gharzouni[1] · E. Joussein[2] · M. Colas[3] · J. Cornette[3] · J. Absi[3] · S. Rossignol[1]

Received: 20 January 2017 / Accepted: 19 April 2017

Abstract Alkaline silicate solutions are used for different industrial applications. Structural studies of these solutions performed by fourier transform infrared and nuclear magnetic resonance spectroscopies have shown the presence of cyclic species. However, these techniques do not allow determining the variations of chain and ring size depending on the content of alkali cations and water. The objective of this study was thus to use Raman spectroscopy to obtain additive information, such as variations of ring and chain size to evaluate the reactivity of the silicate solutions. For this, several solutions were prepared according to different preparation methods (commercial or laboratory) with different cations and Si/M ratios (M = Na and/or K). The structural results obtained by Raman spectroscopy showed that the preparation method has an effect on the variation of the amount of rings with 3 and 4 tetrahedra. It has also been demonstrated that the cation had a stronger influence on the variations of these rings for commercially available solutions compared to their laboratory-made counterparts. Moreover, in the case of mixed solutions (M = Na + K), the alkali cation influenced the formation of this type of rings. Then, the effect of the Si/M ratio on the different species was highlighted and, in particular, the formation of rings at the expense of chains. Finally, this study has demonstrated that Raman spectroscopy is a crucial technique for understanding the structure of silicate solutions and their reactivity.

Graphical Abstract

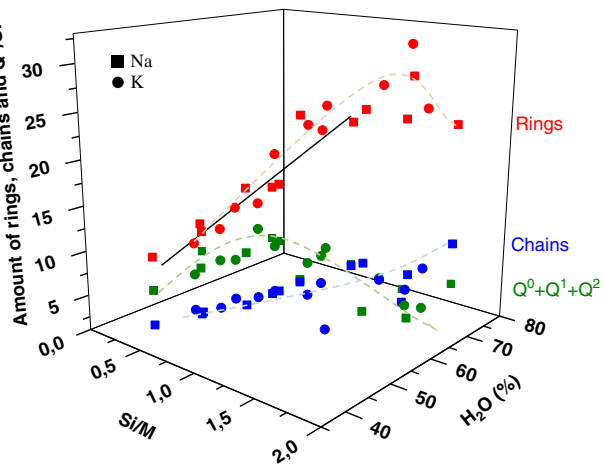

Keywords Silicate solution · Alkaline nature · Polymerization degree · Raman spectroscopy · Reactivity · Alkali concentration

1 Introduction

Alkaline silicate solutions (also called water glass) are part of the silicate family. These solutions can be used in many industrial applications including binders, gel formers,

Electronic supplementary material The online version of this article (doi:10.1007/s10971-017-4394-z) contains supplementary material, which is available to authorized users.

✉ S. Rossignol
sylvie.rossignol@unilim.fr

[1] SPCTS, ENSCI, 12 rue Atlantis, 87068 Limoges CEDEX, France

[2] Université de Limoges, GRESE EA 4330, 123 avenue Albert Thomas, 87060 Limoges, France

[3] Université de Limoges, SPCTS, 12 rue Atlantis, 87068 Limoges CEDEX, France

Published online: 02 May 2017

coatings, deflocculants, or corrosion inhibitors [1, 2]. For the last few decades, they have also been used as binders for the agglomeration of sand in the electrical industry [3, 4] and as reagents for the production of geopolymers [5]. The solutions used for these two applications do not have the same characteristics with regard to the water content and the Si/M molar ratio (M = Na or K). Thus, for the agglomeration of sand, the solutions are used as they are, while in the case of geopolymers, the Si/M ratio of commercially available solutions is reduced with alkali hydroxides. The various applications for which these solutions are employed will depend on their reactivity based on the cation M and the water content.

To understand the above-mentioned parameters, several authors have conducted structural studies with fourier transform infrared (FTIR) and ^{29}Si nuclear magnetic resonance spectroscopies (NMR) [2, 6]. It was shown that the degree of polymerization depends on the Q^n species distribution [7, 8]. The used method to prepare the solution has an effect on the silicate species. Several authors [9–11] have demonstrated that, for the same Si/M ratio, a commercial silicate solution in which KOH pellets were dissolved and a laboratory solution have the same silicate species in different amounts. Moreover, the preparation method results in the presence of Q^n species in different amounts and higher water content promotes the polymerization of the solution [3].

The alkali cation has also a slight influence on the silicate species. Increasing the size of the cation promotes the formation of silicate species that are slightly more polymerized as well as Q^{2c} and Q^{3c} species [7, 12]. This phenomenon is due to the fact that the hydration shell radius decreases as the cation size increases. Mähler and Persson [13] estimated the radius of the Na^+ and K^+ cations and showed that the Na–O distance was slightly smaller than the K–O distance. According to Melkior et al. [14], the potassium cation has a faster diffusion rate than its sodium counterpart due to the Stokes radius of the cation. For high Si/M ratios, the solutions contain predominantly Q^2 and Q^3 species associated with Q^4 entities in small quantities [8, 15]. A decrease of the Si/M ratio leads to the formation of Q^0 and Q^1 species associated with the appearance of cyclic Q^{2c} and Q^{3c} species for Si/M ratios smaller than 1 [16, 17], thus promoting depolymerization. Consequently, several parameters can be used to control the degree of polymerization and therefore the reactivity of the silicate solutions. Consequently, studies using FTIR spectroscopy [18, 19] and NMR ^{29}Si [18, 20] on silicate glass have therefore assessed the changes in Q^n species as a function of the alkali content [21] as well as the presence of monomers and oligomers [22].

To supplement these data, Raman spectroscopy could be a useful complementary technique. Indeed, studies on glass samples have shown that Raman spectroscopy can give informations on the size of the rings and on the Q^n species distribution [23, 24]. Nevertheless, few authors report some studies on silicate solutions [25–27]. Contributions attributed to ring breathing mode as well as the vibration of the monomers and oligomers, and their variations as a function of the Si/M ratio have been observed [25, 26]. Indeed, an increase in the quantity of alkali cations was found to lead to an increase in three-memberred rings and monomers, associated with a reduction in four-membered rings and oligomers [25, 28]. Trcera [29] noted a shift to higher wavenumbers of the band attributed to the rings with five tetrahedra or more when the amount of alkali ions increased. This shift has been linked to a reduction of the Si–O–Si angles and thus to a decrease in the size of the rings in accordance with the work by Galeener [24]. Furthermore, a study has shown that increasing the water content in sodium-silicate glass leads to the disappearance of the three-membered rings [30]. Depolymerization phenomena have also been seen thanks to the variations in the Q^n silicate species distribution. Indeed, increasing the quantity of alkali cations led to reduced Q^4 species in favor of Q^3 species [23, 26]. For higher amounts of alkali cations, the formation of Q^2 entities at the expense of Q^3 species was observed, indicating a depolymerization phenomenon.

Variations of the different Q^n species cannot be correlated to the reactivity of the silicate solutions [6, 26]. Indeed, a previous study showed a maximal reactivity for Si/M ratios between 0.5 and 1.0 [23]. However, the presence of only cyclic species was noted for this range of Si/M ratios [6, 26]. Raman spectroscopy could thus be used to determine the reactivity (or attack capability) of the solutions.

The aim of this work is to perform Raman analysis on various silicate solutions, at room temperature, in order to identify the presence of chains and rings to determine the reactivity of the solutions. Various parameters were studied, such as the preparation mode (commercial or laboratory), the alkali cation (K, Na and NaK mixture) and the Si/M ratio (from 0.2 to 1.7). These parameters were systematically compared as a function of the different contributions determined from the spectra.

2 Materials and methods

2.1 Raw materials and sample preparation

Various potassium, sodium or mixed (K and Na) silicate solutions were used for this study and are presented in Table 1. The parameters studied were the alkali cation (K and/or Na), the Si/M molar ratio with M = K and/or Na (from 0.2 to 1.7) and the manufacturing process. In order to study the influence of this process, commercially available and lab-prepared solutions were used. The commercial

Table 1 Characteristics and nomenclature of the studied K-based solutions (C = commercial, L = laboratory)

Cation	Manufacturing method	Si/M	Nomenclature	Symbols
K	Laboratory	1.7	$_{L}K^{1.7}$	◇
	Commercial	1.7	$_{C}K^{1.7}$	□
		1.5	$_{C}K^{1.5}$	
	Laboratory	1.4	$_{L}K^{1.4}$	◇
		1.0	$_{L}K^{1.0}$	
	Commercial		$_{C}K^{1.7}{}_{K}1.0$	×
	Laboratory	0.7	$_{L}K^{0.7}$	◇
	Commercial		$_{C}K^{0.7}$	□
		0.6	$_{C}K^{1.7}{}_{K}0.6$	×
		0.5	$_{C}K^{1.5}{}_{K}0.5$	
			$_{C}K^{0.7}{}_{K}0.5$	
			$_{C}K^{0.5}$	□
	Laboratory		$_{L}K^{0.5}$	◇
		0.35	$_{L}K^{0.35}$	
		0.2	$_{L}K^{0.2}$	

The characteristics for the other solutions are reported in the supplementary file A

silicate solutions were supplied by the companies Woellner[1] and MERSEN[2]. The lab-prepared solutions were obtained by the dissolution of KOH or NaOH pellets (85.2% and 97% purity, respectively) and amorphous silica (99.9% purity) in osmotically purified water at room temperature, as described elsewhere [5]. To compare the various solutions, MOH pellets (M = K or Na) were dissolved in the commercially available or laboratory-made solutions. The nomenclature used for these different solutions is listed in Table 1 and can be seen in Fig. 1.

For the commercially available solutions, the nomenclature was $_{C}M^{x}$, where M denoted the alkali cation (Na and/or K), x was the Si/M molar ratio (from 0.2 to 1.7) and C stood for commercial. For example, a commercially available potassium-based silicate solution with a Si/M ratio equal to 1.7 was named $_{C}K^{1.7}$. Concerning the lab-prepared solutions, the nomenclature used was $_{L}M^{x}$, where M denoted the alkali cation (Na or K), x was the Si/M ratio (from 0.2 to 1.7), and L stood for laboratory. For example, a lab-prepared sodium-based silicate solution with a Si/M ratio equal to 0.5 was called $_{L}Na^{0.5}$. Finally, the mixed solutions were given the designation $_{z}M^{x}{}_{M}{}^{y}$, where M denoted the alkali cation (M = K and/or Na), z described the manufacturing process (z = C for commercial or L for laboratory), x was the initial Si/M molar ratio (from 0.7 to 1.7), and y corresponded to the final Si/M molar ratio (from 0.2 to 1.0). For example, a lab-prepared sodium-based silicate solution, with an initial Si/M molar ratio of 1.7, in which KOH pellets were added to obtain a final Si/M molar ratio equal to 0.5 was named $_{L}Na^{1.7}{}_{K0.5}$. A commercial potassium-based silicate solution, with an initial Si/M molar ratio of 0.7, in which NaOH pellets were added to obtain a final Si/M molar ratio equal to 0.5 was called $_{C}K^{0.7}{}_{Na0.5}$.

[1] Woellner GmbH, Wöllnerstraße 26, D-67065 Ludwigshafen, Germany.

[2] MERSEN, 15 Rue Jacques Vaucanson, 69720 St Bonnet de Mure Cedex, France.

2.2 Sample characterization

Raman spectroscopy was performed on liquid samples using a T64000 Horiba-Jobin-Yvon spectrophotometer with a 514-nm laser excitation operating at a power of 30 mW at the sample in the triple substractive mode using 1800 grooves per mm grating. Scattered light was collected in backscattering mode using a specific "pseudo-macro" stage for liquid samples. The spectral range was 300 to 1300 cm^{-1}, and 60 scans of 15 s each were carried out for the acquisition. The obtained Raman spectra are displayed in the supplementary file B. To be closer to the raw data, no smoothing processing was applied to the various Raman spectra. The subtracted baseline was modeled by a 5°-polynomial curve. Then, Raman spectra were decomposed by pseudo-Voigt function using least square minimization (Wire 4.0 software). In order to avoid the broadening of the bands, the position and the width of the various contributions were constrained (Appendix). The various contributions identified by Raman spectroscopy are listed in Table 2, and Raman spectra obtained for $_{L}K^{0.7}$ and $_{L}Na^{0.7}$ solutions are presented in Fig. 2. It can be seen that the used method for collecting Raman spectra made it possible to identify the various contributions.

3 Results and discussions

3.1 Decomposition of the Raman spectra—effect of Si/M molar ratio

In order to determine each contribution, such as monomers and rings, from the various silicate solutions, the Raman spectra have been decomposed taking into account the literature data of the frequencies attributions (Table 2) and the previous paper by Vidal et al. [26] regarding silicate solutions. To determine the effect of the Si/M molar ratio and the alkali cation on the polymerization of the silicate species present in the solutions, spectra of six laboratory-made Na-silicate and K-silicate solutions with varying Si/M ratios ($_{L}K^{1.7}$, $_{L}K^{1.0}$, $_{L}K^{0.5}$, $_{L}Na^{1.7}$, $_{L}Na^{1.0}$ and $_{L}Na^{0.5}$, see nomenclature in Table 1 and in the appendix) were studied (Fig. 3 and Table 3). For a Si/M ratio = 1.7 ($_{L}K^{1.7}$), the decomposed Raman spectrum showed contributions due to

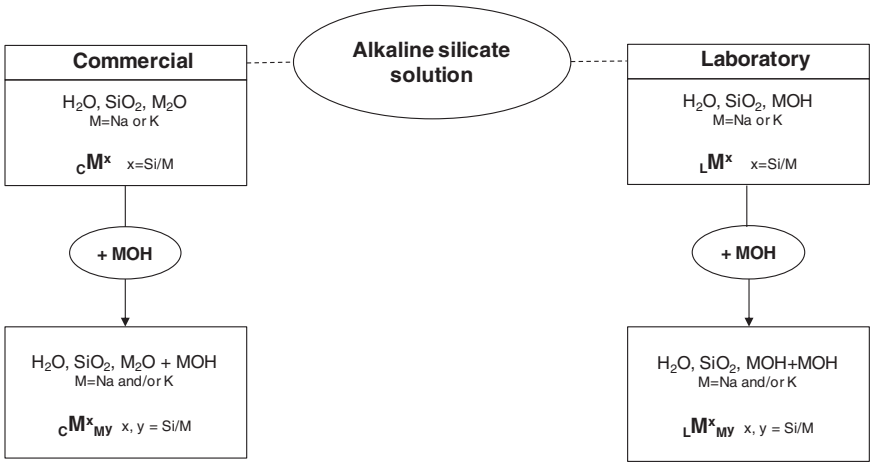

Fig. 1 Schema presenting the various alkaline silicate solutions studied and their nomenclatures

the stretching of Q^1 ($SiO_{1/2}O_3^{3-}$), Q^2 ($SiO_2O_2^{2-}$), Q^3 ($Si_2O_{3/2}O^-$), and Q^4 (SiO_4) species, which can be evidenced near 875, 1000, 1060, and 1120 cm^{-1}, respectively [25, 27, 31] (Fig. 3). Weak contributions attributed to the bending of M–O bonds and to the longitudinal and transverse optical (LO/TO) vibration modes were observed at 320 and 785 cm^{-1}, respectively [32, 33]. Finally, all the contributions in the low-wavenumber range (300–700 cm^{-1}) were effective. For example, the bands observed near 440, 550, 600, 500, and 645 cm^{-1} were attributed to the ring breathing mode of the ring with five or more tetrahedra (denoted $\delta[R_{5\text{ or more}}]$), to $\delta[R_3]$ (three-membered rings), to $\delta[R_4]$ (four-membered rings), to the stretching of ν_S(Si–O–Si) of the chains ($C_{5,6,7}$) and to monomer contributions, (ν_S(Si-O)), respectively[20, 23, 34, 35]. The curve-fitting results of the Raman spectra are reported in Table 3 and show that, regardless the alkali cation, the same contributions were identified with variable areas. Nevertheless, the cation effect on the contribution area was relatively limited when the Si/M ratio was high (Si/M > 1). However, the presence of Q^3 and Q^4 contributions were proof that the solution was polymerized, which is consistent with previous results by Vidal et al. [26].

For the solution with a Si/M ratio equal to 1 ($_LK^{1.0}$), changes were clearly effective. Indeed, all the contributions seem to be more intense than for the $_LK^{1.7}$ (Supplementary file). Moreover, the Q^4 band disappeared, whereas a band near 830 cm^{-1} attributed to Q^0 species was observed. The disappearance of the contribution from the Q^4 species highlights a less significant polymerization state compared to the $_LK^{1.7}$ and $_LNa^{1.7}$ solutions. Equivalent contributions were observed in the low-wavenumber range (see Table 3 and previous results). Globally, the curve fitting gives evidence of an increase in the area of the $\delta[R_{3,\ 4}]$ and M–O with the decrease of the Si/M ratio for both cations. The contributions attributed to the Q^2 and Q^3 species appeared to be more intense for low Si/M ratios (Si/M < 1). However, it seemed that these latter species were more pronounced in the case of the K-based silicate solution compared to its Na-based counterpart (Table 3). Moreover, an increased content of alkali cation led to a decrease of the TO/LO and $C_{5,6,7}$ contributions, indicating that these solutions were less polymerized. The decrease of the Si/M molar ratio to 0.5 ($_LK^{0.5}$ and $_LNa^{0.5}$) led to an increase of the Q^0, Q^1, and Q^2 bands to the detriment of the Q^3 contribution. Moreover, in the low-wavenumber range, the contributions attributed to $\delta[R_{3,\ 4}]$ decreased. The relative intensity of the $\delta[R_{5\text{ and more}}]$ and M–O contributions were exacerbated in the case of the solution with a Si/M ratio = 0.5, which suggests that the M–O bonds may be associated with the monomers for low Si/M ratios, i.e., for very depolymerized solutions. This fact reveals that the solutions were highly depolymerized. Moreover, the contributions attributed to Q^0 and Q^1 silicate species were slightly more pronounced for $_LNa^{0.5}$ than for $_LK^{0.5}$. This fact highlights that sodium silicate solutions may be slightly more depolymerized than their potassium

Table 2 Vibrational wavenumbers of silicate species for Raman spectroscopy

Contribution	Raman shift (cm^{-1})	References
ν_s (Si–O) (Q^4)	1120–1230	[30, 33]
ν_s (Si–O^-) (Q^3)	1000–1100	[16, 30]
ν_s (Si-O^-) (Q^2)	920–1000	[14, 16]
ν_s (Si–O^-) (Q^1)	850–920	[35]
ν_s (Si–O^-) (Q^0)	800–875	[34, 35]
TO/LO (Si–O–Si)	650–850	[35]
ν_s (Si–O) (monomers)	639–649	[36]
D_2 (δ [R_3])	587–606	[14, 32]
ν_s (Si–O–Si) ($C_{5,6,7}$)	515–535	[36]
D_1 (δ [R_4])	453–550	[10, 32]
δ [$R_{5\text{ or more}}$]	400–490	[10, 34]
M–O (network modifiers)	340–360	[34]

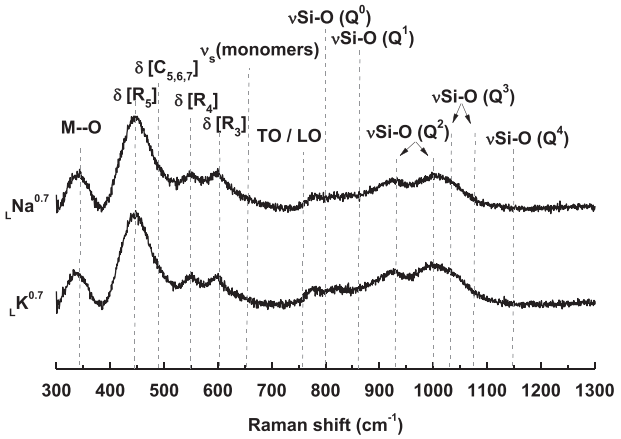

Fig. 2 Raman spectra of $_{L}K^{0.7}$ and $_{L}Na^{0.7}$ solutions

silicate counterparts. The increased amount of oligomer species with the decrease of the Si/M ratio may be an important factor concerning the attack capacity of the silicate solutions.

3.2 Effect of alkali cation amount and nature

In order to investigate the effect of alkali cation amount and nature in the distribution of silicate species obtained by Raman spectroscopy, the variation of M–O, $R_{5\ or\ more}$, R_4, R_3 and $C_{5,6,7}$ species contribution areas were plotted as a function of the alkali cation amount (alkali cation concentration divided by the M–O distance, which is the distance between the alkali cation and the non-bridging oxygen atom) (Fig. 4). Figure 4a shows the percentage of the M–O contribution, as a function of the alkali cation amount and nature. To evaluate its influence, the alkali cation amount was expressed in concentration divided by the M–O distance in order to take into account the difference of cation nature (potassium, sodium). Regardless the cation and the solution in question, there was an increase in the M–O contribution when the content of alkali cation increased; however, the variation was not linear over the considered concentration range. It increased linearly for an alkali cation amount ranging from 0.5 to about 4 a.u., then leveled off for higher concentrations. Indeed, for the solutions $_{C}K^{x}$ and for a concentration of approximately 0.7 a.u. ($_{L}K^{1.7}$), the M–O contribution was about 7% whereas for a concentration close to 4 a.u. ($_{C}K^{0.5}$), the contribution increased to 24%. This phenomenon was also observed for $_{L}Na^{x}$ solutions where the M–O contribution varied from 5 to 22% for concentrations ranging from 1 to 4 a.u.. Subsequently, this contribution remained constant at about 25% for concentrations greater than 4.5 a.u.. The existence of a plateau can be correlated with a state of complete dissociation of the siliceous species [8]. Indeed, when the M–O content was

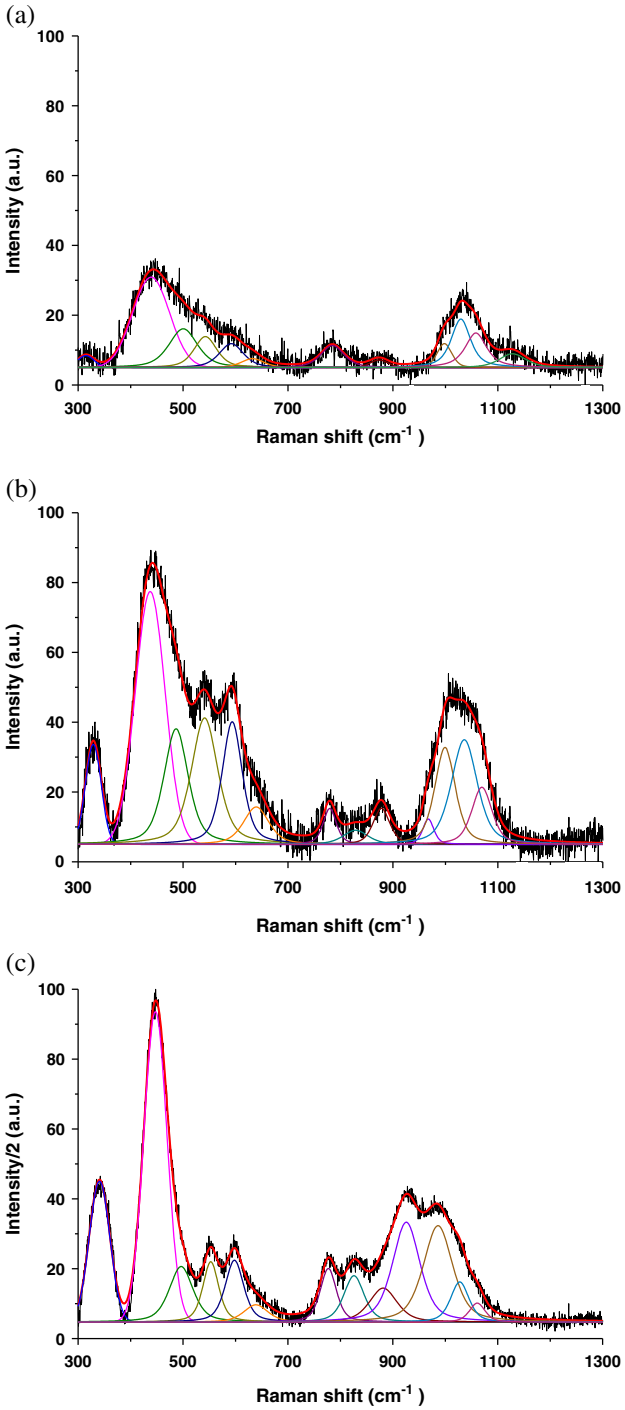

Fig. 3 Curve-fitting of Raman spectra for **a** $_{L}K^{1.7}$, **b** $_{L}K^{1.0}$ and **c** $_{L}K^{0.5*}$ solutions based on potassium (*Intensity divided by 2)

stable, the silicate species were completely dissociated. According to pH measurements (previously made at the laboratory), this complete dissociation was due to pH values of 14 or higher and Si/M ratios below 0.5. Indeed, for Si/M ratios below 0.5, highly depolymerized species (Q^0) predominated. Svensson et al. [10] have demonstrated that for

Table 3 Curve-fitting results of Raman spectra of some silicate solutions (a) in 300–700 cm^{-1} and (b) in 700–1200 cm^{-1} wavenumber range

		Raman contributions							
		Area (%) (±2%) [Position (cm^{-1}) (±2.5 cm^{-1})]							
		M–O	δ [$R_{5\ or\ more}$]	ν_s (Si–O–Si) ($C_{5,\ 6,\ 7}$)	D_1 (δ [R_4])	D_2 (δ [R_3])	ν_s (Si–O) (monomers)		
(a)									
Solution	$_LK^{1.7}$	2.9 (315)	49.5 (439)	20.5 (500)	12.9 (543)	10.6 (592)	3.6 (633)		
	$_LNa^{1.7}$	5.1 (326)	49.2 (440)	18.6 (504)	12.3 (550)	9.6 (600)	5.2 (644)		
	$_CNa^{1.35}$	7.4 (329)	44.1 (445)	6.5 (498)	16.6 (539)	20.4 (595)	5.0 (655)		
	$_LNa^{1.35}$	7.7 (331)	39.0 (440)	15.2 (495)	16.6 (540)	15.8 (595)	5.7 (645)		
	$_LK^{1.0}$	7.5 (329)	36.0 (437)	16.6 (487)	19.8 (541)	14.5 (594)	5.6 (639)		
	$_LNa^{1.0}$	11.3 (331)	35.2 (443)	13.7 (497)	16.5 (545)	15.5 (595)	7.8 (643)		
	$_CK^{0.7}$	12.7 (335)	42.5 (445)	12.6 (499)	11.6 (549)	14.9 (596)	5.7 (640)		
	$_LK^{0.7}$	20.5 (333)	44.1 (445)	9.4 (496)	8.5 (547)	8.7 (593)	8.8 (620)		
	$_LK^{0.5}$	19.5 (341)	48.3 (447)	11.1 (497)	8.0 (553)	9.6 (598)	3.5 (639)		
	$_LNa^{0.5}$	21.9 (343)	45.8 (447)	10.5 (501)	7.0 (555)	9.2 (597)	5.6 (642)		
	$_LK^{1.7}{}_{Na}{}^{0.5}$	19.7 (342)	45.7 (446)	11.8 (492)	10.0 (552)	9.7 (600)	3.1 (643)		
	$_LNa^{1.7}{}_{K}{}^{0.5}$	18.1 (341)	46.3 (446)	12.7 (491)	12.1 (555)	4.7 (598)	6.1 (628)		
	$_LK^{0.7}{}_{Na}{}^{0.5}$	22.1 (339)	45.3 (446)	11.4 (490)	8.8 (553)	4.7 (597)	7.7 (624)		
	$_LNa^{0.7}{}_{K}{}^{0.5}$	20.0 (342)	46.5 (447)	9.9 (495)	10.5 (553)	7.8 (599)	5.3 (640)		
(b)									
		TO/LO (Si–O–Si)	ν_s (Si–O^-) (Q^0)	ν_s (Si–O^-) (Q^1)	ν_s (Si–O^-) (Q^{2c})	ν_s (Si–O^-) (Q^2)	ν_s (Si–O^-) (Q^{3c})	ν_s (Si–O^-) (Q^3)	ν_s (Si–O) (Q^4)
Solution	$_LK^{1.7}$	16.4 (785)	–	3.8 (874)	–	10.4 (998)	31.7 (1029)	25.9 (1058)	11.8 (1128)
	$_LNa^{1.7}$	22.6 (786)	–	4.9 (880)	–	9.7 (993)	33.1 (1026)	17.6 (1057)	12.1 (1123)
	$_CNa^{1.35}$	4.3 (782)	6.2 (859)	13.1 (892)	–	27.4 (987)	31.4 (1027)	12.2 (1065)	5.4 (1123)
	$_LNa^{1.35}$	10.8 (784)	2.7 (825)	4.6 (872)	–	23.4 (1001)	39.9 (1041)	9.4 (1073)	9.2 (1119)
	$_LK^{1.0}$	6.4 (779)	4.7 (829)	8.0 (878)	3.7 (967)	26.3 (999)	35.6 (1036)	15.3 (1070)	–
	$_LNa^{1.0}$	3.7 (779)	8.3 (838)	16.6 (883)	5.4 (960)	20.9 (991)	24.9 (1026)	20.2 (1064)	–
	$_CK^{0.7}$	5.8 (778)	7.7 (824)	16.0 (878)	14.0 (917)	30.2 (993)	20.6 (1034)	5.7 (1063)	–
	$_LK^{0.7}$	6.4 (775)	16.8 (822)	12.1 (882)	14.2 (921)	40.5 (994)	6.8 (1032)	3.2 (1066)	–
	$_LK^{0.5}$	9.3 (777)	10.1 (826)	10.0 (882)	29.3 (926)	30.2 (986)	7.9 (1028)	3.2 (1061)	–
	$_LNa^{0.5}$	7.9 (776)	15.8 (829)	15.2 (896)	28.4 (933)	22.8 (985)	6.5 (1022)	3.4 (1053)	–
	$_LK^{1.7}{}_{Na}{}^{0.5}$	7.3 (777)	13.8 (824)	13.5 (891)	25.4 (927)	26.3 (984)	7.8 (1018)	5.9 (1046)	–
	$_LNa^{1.7}{}_{K}{}^{0.5}$	6.9 (777)	14.5 (825)	12.0 (892)	27.7 (931)	26.6 (990)	8.9 (1022)	3.4 (1066)	–
	$_LK^{0.7}{}_{Na}{}^{0.5}$	9.4 (778)	11.0 (827)	12.9 (887)	28.2 (930)	27.7 (991)	7.5 (1028)	3.3 (1065)	–
	$_LNa^{0.7}{}_{K}{}^{0.5}$	8.0 (777)	13.5 (825)	10.5 (886)	28.8 (927)	28.3 (985)	7.6 (1025)	3.3 (1061)	–

–, no contribution

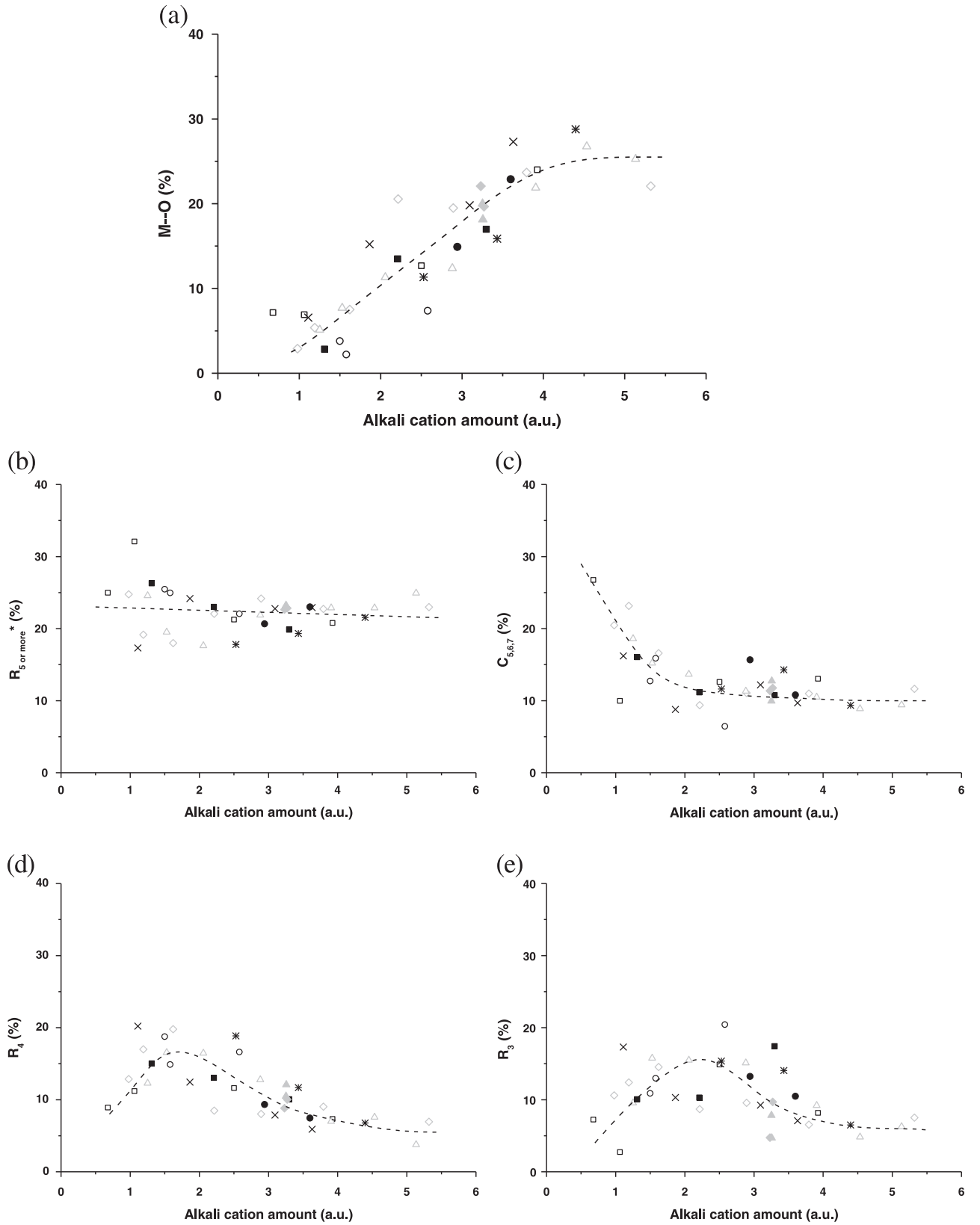

Fig. 4 Variation of the contributions areas relative to **a** M–O, **b** $R_{5\ or\ more}$*, **b** $C_{5,6,7}$, **c** R_4 and **d** R_3 as a function of the alkali cation amount for (□) ${}_{C}K^{x}$, (○) ${}_{C}Na^{x}$, (◇) ${}_{L}K^{x}$, (△) ${}_{L}Na^{x}$, (✕) ${}_{C}K^{x}{}_{K}{}^{y}$, (✻) ${}_{C}Na^{x}{}_{Na}{}^{y}$, (■) ${}_{C}K^{x}{}_{Na}{}^{y}$, (●) ${}_{C}Na^{x}{}_{K}{}^{y}$, (◆) ${}_{L}K^{x}{}_{Na}{}^{y}$ and (▲) ${}_{L}Na^{x}{}_{K}{}^{y}$ (* area divided by 2) (±2%)

low SiO_2/M_2O ratios, the predominate silicate species were Q^0 entities. Other authors have also observed these changes [15, 18]. The change in the M–O contribution seems to depend on the water amount and the alkali cation content. The reactivity of silicate species and thus silicate solutions can be controlled by knowledge of the alkali cation, the preparation method and the water content of these solutions to determine a tendency curve of the reactivity of the silicate species.

The contributions attributed to rings with five or more tetrahedral ($R_{5\ or\ more}$) (Fig. 4b) remained constant with high amount when the alkali cation content increased in the studied Si/M domain, whereas contribution area relative to $C_{5,6,7}$ decreased and then stabilized (Fig. 4c).

Thus, for high Si/M ratios, very large rings would be present and a decrease in the Si/M ratio induces the formation of smaller rings, such as R_5. This part will be discussed later.

The R_4 and R_3 species (Fig. 4d, e) had the same variations, namely an increase to a concentration of between 1.5 and 2 a.u. followed by a decrease. However, the maximum was reached at different alkali amounts (1.5 and 2 a.u. for the R_4 and R_3 contributions, respectively). The R_4 rings decreased at slightly lower concentrations than their R_3 counterparts (1.5 and 2 a.u. for respectively the R_4 and R_3 rings). Indeed, these rings would be transformed faster than the rings of smaller size because of steric hindrance. The small amount of rings at low concentrations could be due to the large amount of water in these solutions. Indeed, Zotov et al. [30], have shown that increasing the amount of water in sodium-silicate glass results in the disappearance of the bands attributed to the R_3 rings. This could explain the low amount of rings observed for very low alkali cation amounts (about 1 a.u.). The observed increase in R_3 and R_4 can be correlated to the decrease in chains and was thus due to the closing of chains as soon as the alkali cation was added. Indeed, when the alkali cation concentration increased, the stresses exerted by the cations may become more significant and may promote a folding of the chains onto themselves. This consequently led to ring formation. These phenomena can be explained by the equilibrium of the dissociation of siliceous species [8, 16]. In fact, the solutions with high Si/M ratios contained a majority of Q^3 species, which is consistent with previous findings and the literature [15, 16]. Their presence might be explained by the fact that the solutions contained branched chains based on Q^3. Therefore, when the alkali cation concentration increases, the stresses exerted by the cations may close the chains leading, consequently, to the formation of rings.

The alkali cation may also influence the band's positions. That is why, the evolution of the position of the band attributed to M–O vibration and to ring breathing mode of rings with five tetrahedra or more as a function of the alkali cation amount of the solution was plotted (Fig. 5). A shift of these contributions toward higher wavenumbers occurred as the alkali concentration increased, regardless of the solution under consideration. Indeed, for solution with an alkali concentration near 2 a.u., the M–O band was around 310 cm^{-1} while it was located at about 355 cm^{-1} for a concentration of about 15 a.u. In the case of the $R_{5\ or\ more}$ contribution, the position of this band varies from 437 to 460 cm^{-1} for alkali amounts varying from 2 to 15 a.u. This phenomenon has also been observed in silicate glass [36]. Trcera [29] noticed a shift of the bands attributed to the rings and linked this result to a decrease the Si–O–Si angle values. However, Galeener [24] showed that Si–O–Si angle the values were related to the ring size. Thus, Trcera [29] put forward the theory that the shift of the bands attributed to the rings may be due to the reduction in the size of the latter. Thus, in the case of silicate solutions, the shift of the band associated with $R_{5\ or\ more}$ was consistent with the

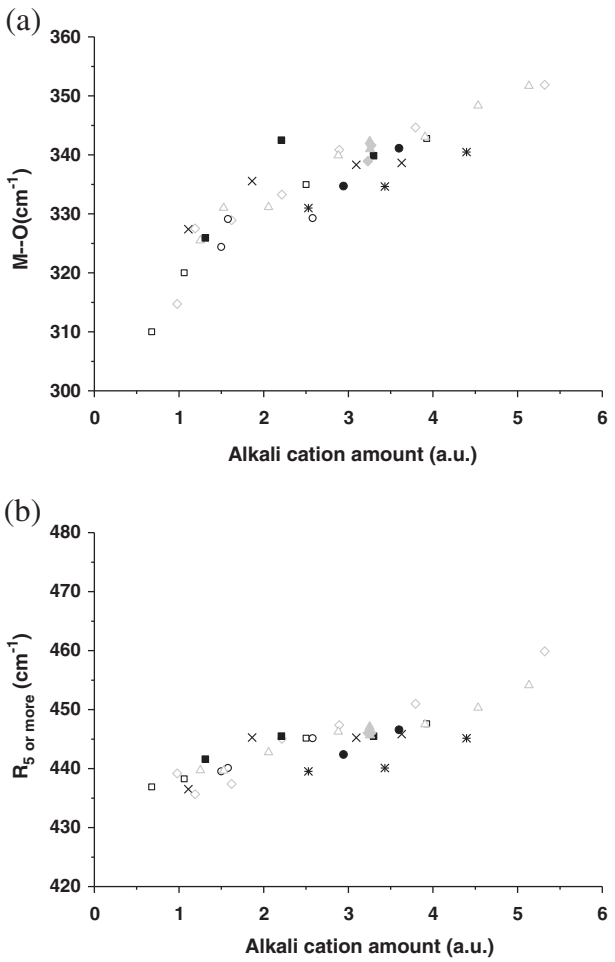

Fig. 5 Variation of the position of the **a** M–O and **b** $R_{5\ or\ more}$ contributions as a function of the alkali cation amount for (□) $_CK^x$, (○) $_CNa^x$, (◇) $_LK^x$, (△) $_LNa^x$, (✕) $_CK^x{}_K{}^y$, (✻) $_CNa^x{}_{Na}{}^y$, (■) $_CK^x{}_{Na}{}^y$, (●) $_CNa^x{}_K{}^y$, (◆) $_LK^x{}_{Na}{}^y$ and (▲) $_LNa^x{}_K{}^y$ (±2.5 cm^{-1})

reorganization of rings corresponding to a reduction of their size. Large rings were broken and smaller rings were formed.

3.3 Effect of manufacturing process

Given these different variations and large concentration ranges, the reactivity of the solutions can be demonstrated by the variation of the rings and chains at a fixed concentration of silicon atoms. The contributions of the chains ($C_{5,6,7}$), rings ($R_3 + R_4 + R_5$) and Q^n species ($Q^0 + Q^1 + Q^2$) for one silicon atom were plotted against the cation nature (Fig. 6). The Q^3 and Q^4 species have not been considered in this section because only the depolymerized Q^n species were taken into account. In this case, regardless of the alkali cation concentration, the same trends were found. Indeed, a significant decrease in rings was observed when the cation concentration increased. In addition, the amounts of chains and Q^n species evolved in an inversely proportional manner. When the chains decreased, an increase in Q^n species was observed. This phenomenon suggests that the chains broke to form more depolymerized entities (Q^0, Q^1 and Q^2). For the laboratory-made solutions at a concentration of 1 a.u., the amount of chains was 8% and the amount of Q^n species was 3%. When the concentration reached 1.5 a.u., the percentage of $C_{5,6,7}$ and Q^n was around 5.5 %. Increasing the concentration to 3 a.u. gave rise to quantities of chains and Q^n species of 8 and 2%, respectively. This phenomenon was also observed with the commercially available solutions, and these developments were consistent with dissociation.

With regard to the variation of the rings, it became more pronounced depending on the preparation method and the alkali cation. Indeed, for the laboratory-made solutions, there was a significant decrease of 30 to 10%, respectively for concentrations of 1 and 5.2 a.u. In addition, sodium-based and potassium-based solutions exhibited similar trends. However, in the case of the commercially available solutions, significant differences were observed for ${}_C K^x$ and ${}_C Na^x$. The number of rings went from 24 to 12% and from 32 to 14%, respectively when the concentration increased from 0.8 to 3.1 and from 1.5 to 3.4 a.u. for the ${}_C K^x$ and ${}_C Na^x$ solutions. The variation in the rings was, as before, certainly due to the dissociated siliceous species. The rings broke when the amount of alkali cations increased.

Regardless of the preparation method, the same quantity of rings was obtained at lower concentrations for the potassium-based solutions compared to those based on sodium. However, this phenomenon was more pronounced in the case of the commercially available solutions. Thus, in commercial solutions, in order to obtain 23% of chains, concentrations of 1.0 and 2.5 a.u. were required respectively for the ${}_C K^x$ and ${}_C Na^x$ solutions. The fact that the same

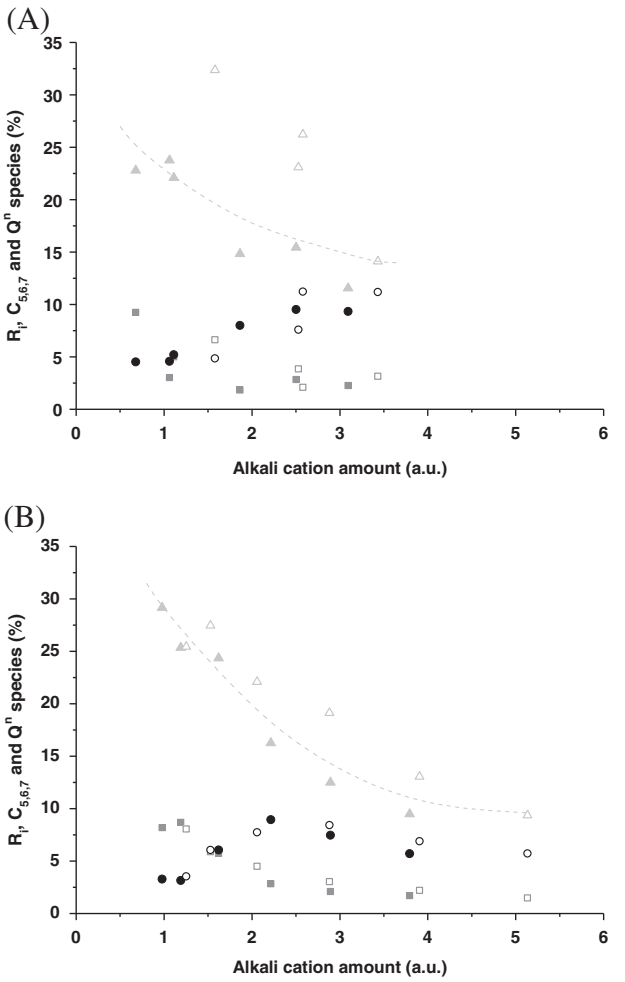

Fig. 6 Variation of the amount of (■) chains ($C_{5,6,7}$), (▲) rings ($R_3 + R_4 + R_5$) and (●) Q^n species ($Q^0 + Q^1 + Q^2$) vs. the alkali cation amount for (A) commercial ${}_C M^x{}_M{}^y$ and (B) laboratory ${}_L M^x{}_M{}^y$ solutions with M = (■, ▲, ●) K or (□, △, ○) Na

number of rings were obtained at a lower concentration for potassium as opposed to sodium may be due to the size of the cation [13] as well as the diffusion rate [14]. Thus, potassium would give rise to a faster formation of rings by forcing chains to close at lower concentrations due to its rapid diffusion. Then, the K^+ cation, which has a greater radius than its sodium counterpart would lead to the destruction of the rings in favor of more depolymerized Q^n species. In the case of sodium, the same phenomena would occur due to the slower diffusion of the cation and its smaller radius. Thus, the diffusion speed and the size of the alkali cation appear to have an influence on the depolymerization phenomena of the solutions.

In addition, the results suggest that commercially available and laboratory-made silicate solutions present differences in reactivity for concentrations between 2 and 4 a.u. These differences were not observed by ^{29}Si NMR. Therefore, these results show that Raman spectroscopy

makes it possible to understand the depolymerization phenomena involved with different cations and for different alkaline solution when this is not possible by NMR.

4 Conclusion

Various commercially available and laboratory-made alkaline silicate solutions based on potassium, sodium or a mixture of the two were studied by Raman spectroscopy. The results show that:

(1) Increasing the alkali cation amount to 5.5 a.u., i.e., decreasing the Si/M ratio from 1.7 to 0.2 resulted in the depolymerization of the solution. Meanwhile, the contribution of R_3 and R_4 rings went through a maximum for amount of 2 and 1.5 a.u., respectively.

(2) The preparation method (commercial or laboratory) affected the silicate species and especially the R_3 and R_4 rings that were preferentially dependent on the alkali cation for the commercially available solutions. Their reactivity can be identified from the variations in the rings as well as in the Q^0 and Q^4 species.

(3) The nature of the alkali cation had an effect on the formation of the rings, particularly for potassium

Thus, Raman spectroscopy is a promising tool for determining the reactivity of silicate solutions, which greatly contributes to the use of such solutions in numerous applications.

Acknowledgements The authors gratefully acknowledge the FEDER agency, the Limousin regional council, the DIRECCTE agency and the FUI program for their financial support.

Compliance with ethical standards

Conflict of interest The authors declare that they have no competing interests.

References

1. Johnson ACJH, Greenwood P, Hagström M, Abbas Z, Wall S (2008) Aggregation of nanosized colloidal silica in the presence of various alkali cations investigated by the electrospray technique. Langmuir 24:12798–12806
2. Tognonvi MT, Massiot D, Lecomte A, Rossignol S, Bonnet JP (2010) Identification of solvated species present in concentrated and dilute sodium silicate solutions by combined ^{29}Si NMR and SAXS studies. J Colloid Interface Sci 352:309–315
3. Lucas S, Tognonvi MT, Gelet JL, Soro J, Rossignol S (2011) Interactions between silica sand and sodium silicate solution during consolidation process. J Non Cryst Solids 357:1310–1318
4. Tognonvi MT, Soro J, Rossignol S (2012) Physical-chemistry of silica/alkaline silicate interactions during consolidation. Part 1: effect of cation size. J Non-Cryst Solids 358:81–87
5. Autef A, Joussein E, Gasgnier G, Rossignol S (2012) Role of the silica source on the geopolymerization rate. J Non Cryst Solids 358:2886–2893
6. Bourlon A (2011) Physico-chimie et rhéologie des géopolymères frais pour la cimentation des puits pétroliers. PhD Thesis, University of Pierre et Marie Curie
7. Steins P (2014) Influence des paramètres de formulation sur la texturation et la structuration des géopolymères. PhD Thesis, University of Limoges
8. Provis JL, Duxson P, Lukey GC, Separovic F, Kriven WM, van Deventer JSJ (2005) Modeling speciation in highly concentrated alkaline silicate solutions. Ind Eng Chem Res 44:8899–8908
9. Gharzouni A, Joussein E, Samet B, Baklouti S, Pronier S, Sobrados I, Sanz J, Rossignol S (2014) The effect of an activation solution with siliceous species on the chemical reactivity and mechanical properties of geopolymers. J Solgel Sci Technol 73:250–259
10. Svensson IL, Sjöberg S, Öhman L-O (1986) Polysilicate equilibria in concentrated sodium silicate solutions. J Chem Soc, Faraday Trans 1 82:3635–3646
11. Prud'homme E, Autef A, Essaidi N, Michaud P, Samet B, Joussein E, Rossignol S (2013) Defining existence domains in geopolymers through their physicochemical properties. Appl Clay Sci 73:26–34
12. Ray NH, Plaisted RJ (1983) The constitution of aqueous silicate solutions. J Chem Soc Dalton Trans: 475–481
13. Mähler J, Persson I (2012) A study of the hydration of the alkali metal ions in aqueous solutions. Inorg Chem 51:425–438
14. Melkior T, Yahiaoui S, Thoby D, Motellier S, Barthès V (2007) Diffusion coefficients of alkaline cations in Bure mudrock. Phys Chem Earth 32:453–462
15. Weber CF, Hunt RD (2003) Modeling alkaline silicate solutions at 25 °C. Ind Eng Chem Res 42:6970–6976
16. Brykov AS, Danilov VV, Aleshunina EY (2008) State of silicon in silicate and silica-containing solutions and their binding properties. Russ J Appl Chem 81:1717–1721
17. Cody GD, Mysen BO, Lee SK (2005) Structure vs. composition: a solid-state ^{1}H and ^{29}Si NMR study of quenched glasses along the Na_2O-SiO_2-H_2O join. Geochim Cosmochim Acta 69:2373–2384
18. Malfait WJ, Halter WE, Morizet Y, Meier BH, Verel R (2007) Structural control on bulk melt properties: single and double quantum ^{29}Si NMR spectroscopy on alkali-silicate glasses. Geochim Cosmochim Acta 71:6002–6018
19. Mysen BO, Cody GD (2005) Solution mechanisms of H_2O in depolymerized peralkaline melts. Geochim Cosmochim Acta 69:5557–5566
20. Zotov N, Ebbsjö I, Timpel D, Keppler H (1990) Calculation of Raman spectra and vibrational properties of silicate glasses: comparison between $Na_2Si_4O_4$ and SiO_2 glasses. Phys Rev B 60:6383–6397
21. Malfait WJ, Zakaznova-Herzog VP, Halter WE (2007) Quantitative Raman spectroscopy: high-temperature speciation of potassium silicate melts. J Non Cryst Solids 353:4029–4042
22. Aguiar H, Serra J, González P, León B (2009) Structural study of sol-gel silicate glasses by IR and Raman spectroscopies. J Non Cryst. Solids 355:475–480
23. Le Losq C, Neuville DR (2013) Effect of the Na/K mixing on the structure and the rheology of tectosilicate silica-rich melts. Chem Geol 346:57–71
24. Galeener FL (1982) Planar rings in vitreous silica. J Non Cryst Solids 49:53–62
25. Hunt JD, Kavner A, Schauble EA, Snyder D, Manning CE (2011) Polymerization of aqueous silica in H2O-K2O solutions at 25–200 °C and 1 bar to 20 kbar. Chem Geol 283:161–170

26. Vidal L, Joussein E, Colas M, Cornette J, Sanz J, Sobrados I, Gelet JL, Absi J, Rossignol S (2016) Controlling the reactivity of silicate solutions: a FTIR, Raman and NMR study. Colloid Surf A 503:101–109
27. Halasz I, Agarwal M, Li R, Miller N (2010) What can vibrational spectroscopy tell about the structure of dissolved sodium silicates? Microporous Mesoporous Mater 135:74–81
28. Malfait WJ, Zakaznova-Herzog VP, Halter WE (2007) Quantitative Raman spectroscopy: high-temperature speciation of potassium silicate melts. J Non Cryst Solids 353:4029–4042
29. Trcera N (2010) Etude de la structure des verres magnésio-silicatés : approche expérimentale et modélisation. PhD Thesis, University of Paris-Est
30. Zotov N, Keppler H (1998) The influence of water on the structure of hydrous sodium tetrasilicate glasses. Am Mineral 83:823–834
31. Belova EV, Kolyagin YA, Uspenskaya IA (2015) Structure and glass transition temperature of sodium silicate glasses doped with iron. J Non Cryst Solids 423–424:50–57
32. Hehlen B, Neuville DR (2015) Raman response of network modifier cations in alumino-silicate glasses. J Phys Chem B 119:4093–4098
33. M Chligui (2010) Etude des propriétés optiques et mécaniques des verres binaires silicatés d'alcalins lourds. Ph.D. Thesis, University of Orléans
34. Depla A, Verheyen E, Veyfeyken A, Van Houteghem M, Houthoofd K, Van Speybroeck V, Waroquier M, Kirschhock CEA, Martens JA (2011) UV-Raman and 29Si NMR spectroscopy investigation of the nature of silicate oligomers formed by acid catalyzed hydrolysis and polycondensation of tetramethylorthosilicate. J Phys Chem C 115:11077–11088
35. Matos MC, Ilharco LM, Almeida RM (1992) The evolution of TEOS to silica gel and glass by vibrational spectroscopy. J Non Cryst Solids 147–148:232–237
36. Malfait WJ, Zakaznova-Herzog VP, Halter WE (2008) Quantitative Raman spectroscopy: speciation of Na-silicate glasses and melts. Am Mineral 93:1505–1518